Research Article

NEURAL REGENERATION RESEARCH
www.nrronline.org

# Blocking postsynaptic density-93 binding to C-X3-C motif chemokine ligand 1 promotes microglial phenotypic transformation during acute ischemic stroke

Xiao-Wei Cao[1, 2, 3, 4, 5, 6, 7, #], Hui Yang[8, 9, #], Xiao-Mei Liu[10], Shi-Ying Lou[1, 2, 11], Li-Ping Kong[11], Liang-Qun Rong[11], Jun-Jun Shan[11], Yun Xu[1, 2, 3, 4, 5, 6], Qing-Xiu Zhang[1, 2, 3, 4, 5, 6, *]

https://doi.org/10.4103/1673-5374.355759

Date of submission: April 19, 2022

Date of decision: July 21, 2022

Date of acceptance: August 4, 2022

Date of web publication: October 10, 2022

### From the Contents



### Graphical Abstract

***During acute ischemic stroke, Tat-CX3CL1 (357–395aa) blocks the combination of PSD-93 and CX3CL1, inhibits the generation of soluble CX3CL1, and promots phenotypic polarization transformation of microglia from M1 type to M2 type***

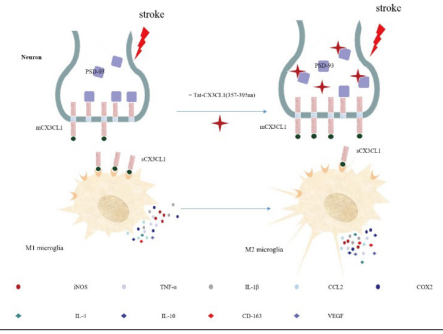


## Abstract

We previously reported that postsynaptic density-93 mediates neuron-microglia crosstalk by interacting with amino acids 357–395 of C-X3-C motif chemokine ligand 1 (CX3CL1) to induce microglia polarization. More importantly, the peptide Tat-CX3CL1 (comprising amino acids 357–395 of CX3CL1) disrupts the interaction between postsynaptic density-93 and CX3CL1, reducing neurological impairment and exerting a protective effect in the context of acute ischemic stroke. However, the mechanism underlying these effects remains unclear. In the current study, we found that the pro-inflammatory M1 phenotype increased and the anti-inflammatory M2 phenotype decreased at different time points. The M1 phenotype increased at 6 hours after stroke and peaked at 24 hours after perfusion, whereas the M2 phenotype decreased at 6 and 24 hours following reperfusion. We found that the peptide Tat-CX3CL1 (357–395aa) facilitates microglial polarization from M1 to M2 by reducing the production of soluble CX3CL1. Furthermore, the a disintegrin and metalloprotease domain 17 (ADAM17) inhibitor GW280264x, which inhibits metalloprotease activity and prevents CX3CL1 from being sheared into its soluble form, facilitated microglial polarization from M1 to M2 by inhibiting soluble CX3CL1 formation. Additionally, Tat-CX3CL1 (357–395aa) attenuated long-term cognitive deficits and improved white matter integrity as determined by the Morris water maze test at 31–34 days following surgery and immunofluorescence staining at 35 days after stroke, respectively. In conclusion, Tat-CX3CL1 (357–395aa) facilitates functional recovery after ischemic stroke by promoting microglial polarization from M1 to M2. Therefore, the Tat-CX3CL1 (357–395aa) is a potential therapeutic agent for ischemic stroke.

**Key Words:** a disintegrin and metalloprotease domain 17; cerebral ischemia/reperfusion; C-X3-C motif chemokine ligand 1; GW280264x; microglia; neuroinflammation; postsynaptic density-93; Tat-CX3CL1 (357–395aa)

## Introduction

Ischemic stroke induces neurotoxicity and neuroinflammation, which are leading causes of death and disability (Jin et al., 2013; Zhang et al., 2014; Rong et al., 2016). In addition, inflammatory responses induced by microglia polarization exacerbate cerebral infarction (Ma et al., 2017). Microglial heterogeneity is of paramount importance for reducing ischemic brain injury, and polarization of microglia toward a M2 phenotype is protective for the brain in the context of ischemic stroke (Wang et al., 2018). However, microglial polarization is highly dependent on environmental signals during cerebral ischemia/reperfusion (Gelderblom et al., 2009; Hu et al., 2015). Therefore, interventions that induce microglia to maintain an M2 phenotype are useful strategies for achieving functional recovery after stroke.

Traditionally, microglia are considered to be tissue-resident macrophages that are specific to the central nervous system (Hu et al., 2015; Gülke et al., 2018). In response to ischemic stroke, microglial cells initiate the production of pro-inflammatory mediators such as interleukin (IL)-1β, tumor necrosis factor (TNF)-α, and IL-6, indicating an M1 phenotype (Hu et al., 2012; Gülke et al., 2018). By contrast, microglia with an M2 phenotype play an anti-inflammatory role by producing anti-inflammatory cytokines, including IL-4, IL-10, and transforming growth factor-β (Hu et al., 2012; Gülke et al., 2018).

[1]Department of Neurology of Drum Tower Hospital, Medical School and the State Key Laboratory of Pharmaceutical Biotechnology, Nanjing University, Nanjing, Jiangsu Province, China; [2]Nanjing Drum Tower Clinical College of Xuzhou Medical University, Nanjing, Jiangsu Province, China; [3]Institute of Brain Sciences, Nanjing University, Nanjing, Jiangsu Province, China; [4]Jiangsu Key Laboratory for Molecular Medicine, Medical School of Nanjing University, Nanjing, Jiangsu Province, China; [5]Jiangsu Province Stroke Center for Diagnosis and Therapy, Nanjing, Jiangsu Province, China; [6]Nanjing Neurology Clinic Medical Center, Nanjing, Jiangsu Province, China; [7]Department of Neurology, Lianyungang Municipal Hospital, Affiliated Hospital of Xuzhou Medical University, Lianyungang, Jiangsu Province, China; [8]Department of Neurosurgery of Drum Tower Hospital, Medical School and the State Key Laboratory of Pharmaceutical Biotechnology, Nanjing University, Nanjing, Jiangsu Province, China; [9]Department of Neurosurgery, Affiliated Xuzhou Municipal Hospital of Xuzhou Medical University, Xuzhou, Jiangsu Province, China; [10]Jiangsu Key Laboratory of Immunity and Metabolism, Department of Pathogen Biology and Immunology and Laboratory of Infection and Immunity, Xuzhou Medical University, Xuzhou, Jiangsu Province, China; [11]Department of Neurology, Second Affiliated Hospital of Xuzhou Medical University, Xuzhou, Jiangsu Province, China

*Correspondence to: Qing-Xiu Zhang, MD, zhangqingxiu@163.com.
https://orcid.org/0000-0001-5285-2908 (Qing-Xiu Zhang)
#These authors contributed equally to this work.

***Funding:*** *This study was supported by the National Natural Science Foundation of China, Nos. 82071304 (to QXZ), 81671149 (to QXZ), and 81971179 (to XML), the Natural Science Foundation of Jiangsu Province, Nos. BK20191463 (to XML) and BK20161167 (to QXZ).*

***How to cite this article:*** *Cao XW, Yang H, Liu XM, Lou SY, Kong LP, Rong LQ, Shan JJ, Xu Y, Zhang QX (2023) Blocking postsynaptic density-93 binding to C-X3-C motif chemokine ligand 1 promotes microglial phenotypic transformation during acute ischemic stroke. Neural Regen Res 18(5):1033-1039.*

In recent years, considerable effort has been devoted to elucidating the role of the microglia phenotypic polarization shift in ischemic brain injury (Liu et al., 2016; Ma et al., 2017; Fumagalli et al., 2018; Wang et al., 2018; Qin et al., 2019).

We previously showed that postsynaptic density-93 (PSD-93) directly binds to amino acids 670–685 of GTPase-activating protein for Ras and promotes GTPase-activating protein for Ras ubiquitination in ischemic brain injury (Zhang et al., 2020). Knocking out PSD-93 improves neurological function by promoting the expression of anti-inflammatory cytokines and inhibiting the expression of pro-inflammatory cytokines (Zhang et al., 2015). Furthermore, we found that PSD-93 interacted with C-X3-C motif chemokine ligand 1 (CX3CL1) to mediate neuron-microglia crosstalk and induce neuroinflammation (Zhang et al., 2021). Using a yeast two-hybrid system and co-immunoprecipitation, we identified the binding sites between these two proteins and constructed a small peptide, Tat-CX3CL1 (357–395aa), which disrupts PSD-93 binding to CX3CL1 and attenuates cerebral infarct volume (Zhang et al., 2021). However, the mechanism underlying this effect remains elusive.

We previously showed that Tat-CX3CL1 (357–395aa) improves functional recovery after ischemic stroke. The aims of the current study were to uncover the mechanism underlying this effect, to determine whether Tat-CX3CL1 (357–395aa) promotes M2 microglia polarization, and to determine whether Tat-CX3CL1 (357–395aa) can improve blood-brain barrier integrity and lead to long-term functional recovery after stroke by promoting microglia polarization.

## Methods

### Animals

A total of 261 C57BL/6 mice (male, 8–10 weeks old, 22–26 g in weight) were purchased from Pengyue Company (Jinan, Shandong Province, China) and maintained on a 12/12-hour light/dark cycle at room temperature (24°C) with *ad libitum* food and water. All animals in this study were specific pathogen-free (SPF) grade, and 3–4 mice were kept in one cage. The study protocols were approved by the Animal Care Committee of Xuzhou Medical University (approval No. 201702w012, approval date: February 12, 2017) and conducted in accordance with international laws and National Institutes of Health policies, including the Guide for the Care and Use of Laboratory Animals (8th ed., National Research Council, 2011). All experiments were designed and reported according to the Animal Research: Reporting of *In Vivo* Experiments (ARRIVE) guidelines (Percie du Sert et al., 2020). Only male mice were used to exclude the effects of estrogen on ischemic injury and stress (Chen et al., 2020). Mice were allocated randomly to the following four groups, with at least five mice in each group, using the random number table method: sham (sham operation), ischemia/reperfusion (I/R; 3, 6, 12, 24, 48, and 72 hours, 7 and 35 days after middle cerebral artery occlusion [MCAO]), Tat-CX3CL1 (MCAO + Tat-CX3CL1 (357–395aa)), and DMSO (MCAO + DMSO [dimethyl sulfoxide]).

### MCAO model

The MCAO model was established as described previously (Zhang et al., 2019). Briefly, mice were anesthetized with ketamine (Cat# K-002, Sigma, St. Louis, MO, USA) and diazepam (Cat# D-907, Sigma) (1:1) (3 mg/kg, i.p.), and the right middle cerebral artery was occluded for 60 minutes. First, we exposed and clipped the right internal common carotid artery. Next, we occluded the right middle cerebral artery by inserting a monofilament into the internal carotid artery and passing it through to the origin of the middle cerebral artery to block the blood flow. After 60 minutes, the monofilament was withdrawn to restore blood flow for the next 3, 6, 12, 24, 48, and 72 hours and 7 and 35 days. In the sham operation group, mice underwent the same surgical procedures except for occlusion of the carotid arteries.

The mortality rate after surgery was 8.05%. All mice that survived were later euthanized by cervical dislocation for analysis. Out of the 261 mice used in this study, 26 were excluded because of failure of ischemia induction (five mice), death (five mice), cerebral hemorrhage (eight mice), and disrupted consciousness (8 mice). A total of 235 mice were included in the final analysis, and there were at least five mice in each group.

### Drug preparation and administration

The peptide Tat-CX3CL1 (357–395 aa) (Cat# 04010055093, China Peptides, Shanghai, China) was synthesized from C-terminus to N-terminus according to the following sequence: 5-FITC-(Acp) MFAYQSLQGCPRKMAGEMVEGLRYVPRSCGSNS YVLVPV. The synthesized peptide was purified to at least 95%, frozen, and powdered for storage. Tat-CX3CL1 (357–395aa) was diluted with DMSO to a concentration of 10 μg/μL, as described previously (Zhang et al., 2021). Mice received intracerebroventricular injections of the diluted peptide or DMSO (negative control) before MCAO and at 1, 2, and 3 days after MCAO (**Figure 1**). The right lateral ventricle was selected for repeated injection of the peptide or DMSO (from the bregma: anteroposterior 1 mm; lateral 1 mm; depth 2 mm; Paxinos and Franklin, 2013).

Mice were randomly assigned to receive either DMSO or the A distintegrin and metalloproteinase (ADAM17) inhibitor GW280264x (Cat# 555806, Medkoo Biosciences, Morrisville, CT, USA) at a concentration of 0.25, 0.5, 1.0, or 1.5 μg/μL by intranasal administration immediately after MCAO surgery (Dreymueller et al., 2012; Zhang et al., 2019). Five 2-μL drops (10 μL total) of GW280264x were applied alternately into each nostril with a 2-min interval between drops. Mice in the control groups received the same volume of DMSO.

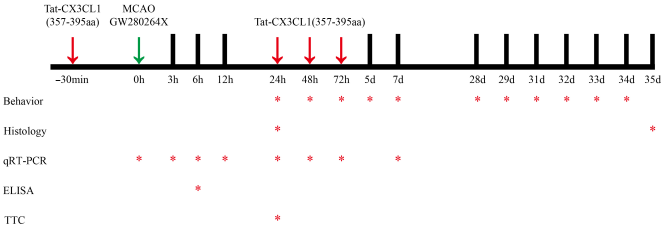


**Figure 1** | **Timeline of the experimental procedures.**
ADAM: A distintegrin and metalloproteinase; ELISA: enzyme linked immunosorbent assay; GW280264x: ADAM17 inhibitor; MCAO: middle cerebral artery occlusion; qRT-PCR: real-time reverse transcription-polymerase chain reaction; TTC: triphenyl tetrazolium chloride.

The mice were treated with Tat-CX3CL1 (357–395 aa) and GW280264x 24 hours after MCAO.

### Triphenyl tetrazolium chloride staining

Triphenyl tetrazolium chloride (TTC) staining was performed as described previously (Zhang et al., 2020). Briefly, 24 hours after MCAO, the mice were euthanized with $CO_2$ and decapitated. The brain slices were stained with 2% TTC (Cat# BCBW4269, Sigma) for 15 minutes at 37°C in the dark.

### Real-time reverse transcription-polymerase chain reaction

Total RNA was extracted from ischemic brain tissue using Trizol (Invitrogen, Carlsbad, CA, USA) and reverse transcribed to cDNA using a cDNA synthesis kit (Takara, Otsu, Japan). The reaction conditions were 95°C for 10 minutes, followed by 40 cycles at 95°C for 15 seconds and 60°C for 60 seconds. The primers were purchased from SANGON Biotech (Shanghai, China) (**Table 1**). The expression levels of target genes were calculated using the $2^{-\Delta\Delta CT}$ method, with glyceraldehyde 3-phosphate dehydrogenase (GAPDH) as an internal control (Zhang et al., 2020). All values are expressed as fold changes *versus* values from the sham group. Statistical analysis was performed to compare the experimental groups to the sham group.

**Table 1** | **Primer sequences used in real-time reverse transcription-polymerase chain reaction**

| Gene | Primer sequence |
|---|---|
| GAPDH | Forward: 5'- GCC AAG GCT GTG GGC AAG GT-3' |
| | Reverse: 5'-TCT CCA GGC GGC ACG TCA GA-3' |
| TNF-α | Forward:5'-TGT GCT CAG AGC TTT CAA CAA-3' |
| | Reverse: 5'-CTT GAT GGT GGT GCA TGA GA-3' |
| IL-10 | Forward:5'-GGC ATG AGG ATC AGC AGG GGC-3' |
| | Reverse:5'-TGG CTG AAG GCA GTC CGC AG-3' |
| iNOS | Forward:5'-CAG CTG GGC TGT ACA AAC CTT-3' |
| | Reverse:5'-CAT TGG AAG TGA AGC GTT TCG-3' |
| CD163 | Forward: 5'-GGG AAG AGT GGA GCT CAA GA-3' |
| | Reverse: 5'-ACC AGC TCC TTT CCC AAA AT-3' |
| IL-1β | Forward: 5'-AAG CCT CGT GCT GTC GGA CC-3' |
| | Reverse: 5'-TGA GGC CCA AGG CCA CAG GT-3' |
| VEGF | Forward: 5'-GGG GAG CAA GCA AGG CCA GG-3' |
| | Reverse: 5'-TCT CTG CCT CCG TGA GGG GC-3' |

GAPDH: Glyceraldehyde-3-phosphate dehydrogenase; IL-10: interleukin-10; IL-1β: interleukin-1β; iNOS: inducible nitric oxide synthase; TNF-α: tumor necrosis factor-α; VEGF: vascular endothelial growth factor.

### Immunofluorescence staining

Brains were removed from mice and fixed in 4% paraformaldehyde at 4°C for 24 hours. The brain tissues were then dehydrated in a 30% sucrose solution for 72 hours and cut into slices (20 μm thick). Sections were blocked with 5% bovine serum albumin (BSA) in PBS containing 0.3% Triton X-100 (PBST) (Solarbio, Beijing, China) at room temperature for 1 hour and then incubated with primary antibodies at 4°C overnight. After washing with PBST, the sections were incubated with specific fluorescent secondary antibodies for 1 hour at room temperature. The sections were observed under a confocal microscope (Leica, Germany). In general, five mice were in each group and three slices analyzed for each mouse, and two fields per section (cortex, striatum, or corpus callosum) were selected for analysis. Positively stained cells were counted by two observers who were blinded to the groups using ImageJ (National Institutes of Health, Bethesda, MD, USA; Schneider et al., 2012).

The following primary antibodies were used: rabbit anti-mouse Iba1 (microglia marker) polyclonal antibody (Cat# 019-19741, Wako, Tokyo, Japan), rat anti-mouse CD68 monoclonal antibody (activated M1 microglia marker) (Cat# ab53444, Abcam, Cambridge, UK), rabbit anti-mouse myelin basic protein (MBP, a major myelin protein) polyclonal antibody (Cat# ab40390, Abcam), and mouse anti-mouse neurofilament H (NF-H) antibody (SMI32, a marker of demyelinated axons) (Cat# 801701, BioLegend, San Diego, CA,

USA). The secondary antibodies used were as follows: Cy3-conjugated goat anti-rabbit IgG (Cat# E031620, Earthox, LLC, San Francisco, CA, USA), Alexa Fluor 488-conjugated donkey anti-rat IgG (Cat# 21208, Invitrogen), and Alexa Fluor 488-conjugated goat anti-mouse IgG (Cat# ab150113, Abcam). Immunofluorescence double-labeling for Iba1 and CD68 was performed 24 hours after MCAO, and immunofluorescence double-labeling for MBP and SMI32 was performed 35 days after MCAO.

**Evaluation of brain water content**

Brain water content was measured using the wet-dry weight method (Qi et al., 2018). Mice were euthanized at 24 hours after MCAO, and the brains were removed quickly and carefully. The wet weight (WW) was measured using an analytical balance (ML204, Mettler Toledo, Switzerland) after removing the olfactory bulbs, cerebellum, and pons. The dry weight (DW) was measured after the brains were baked in an oven at 110°C for 6 hours. Brain water content (%) was determined using the following formula: WC = (WW – DW)/WW × 100.

**Modified neurological function score**

Motor, sensory, reflex, balance, neurological function were evaluated by modified Neurological Severity Score (mNSS) at 1, 3, 5, and 7 days after MCAO, as previously described (Zhang et al., 2020). Total mNSS score were 18 points, and as the score increased, neurological impairment became more severe.

**Morris water maze test**

The Morris water maze test was performed to assess cognitive function, including learning and memory ability, as previously described (Zhang et al., 2019). The Morris water maze (XR-XM101, Xmaze, Shanghai, China) included a circular pool (diameter 120 cm) filled with opaque water, with a square platform (11 cm × 11 cm) submerged 2 cm beneath the water surface. The water temperature was maintained at 21°C. Swimming trajectories were tracked automatically using ANY-maze video tracking software (Stoelting Company, Wood Dale, IL, USA). Briefly, mice were trained in the use of the maze once a day for 3 consecutive days before MCAO, and the experiments were carried out 31–34 days after the MCAO surgery. For the experimental assessment, each mouse was tested four times a day with an interval of 10–15 minutes between tests for 3 consecutive days. The time spent to reach the platform (latency to escape) was recorded. The memory test was performed on day 34 to record the time mice spent in the target quadrant (the quadrant where the platform was originally placed), the number of times the target quadrant was entered, and total swimming distance covered in 1 minute.

**Open field test**

An open field test was performed to evaluate depression 28 days after MCAO, as previously described (Donatti et al., 2017). Briefly, an open box (50 cm × 50 cm × 50 cm) was divided into a peripheral area and a central area. A video monitor was placed above the box to record the frequency with which mice entered the central area and how long they spent there. One week before the experiment, mice were placed in the behavioral test room for 3–5 minutes every day to eliminate fear of the environment and the experimenter. At the beginning of the experiment, mice were gently placed in the box from the edge and allowed to freely explore the open field for 5 minutes. Then, the activity time and number of entries into the central area of the open field were recorded.

**Elevated plus maze test**

An elevated plus maze test was performed 29 days after MCAO to evaluate anxiety based on the contradictory tendencies of mice to explore new environments and to fear the open arm, as previously described (Kraeuter et al., 2019). Briefly, the elevated cross maze consisted of two open arms (50 cm long and 10 cm wide) and two closed arms. The four arms were connected by a central, open platform that was 10 cm × 10 cm in size. The mice were placed on one of the open arms at the beginning of the experiment, and each animal was placed in the same position thereafter. The number of entries and the time spent in each arm were recorded for 5 minutes.

**Enzyme-linked immunosorbent assay**

Soluble CX3CL1 was detected using an enzyme-linked immunosorbent assay (ELISA) kit (R&D Systems, Stillwater, MN, USA) following the manufacturer's instructions. Briefly, mouse brain tissue obtained at 6 hours after stroke was washed with 1× PBS and then homogenized in 5–10 mL of 1× PBS. The homogenate was centrifuged at 5000 × *g* for 5 minutes. Supernatant was analyzed with a Fractalkine ELISA kit. The measured value was 14 ng/mL.

**Statistical analysis**

No statistical methods were used to predetermine sample sizes; however, our sample sizes are similar to those reported in a previous publication (Zhang et al, 2020). In this study, mNSS scores and histological changes were obtained by blinded assessment. Data are shown as mean ± standard error of the mean (SEM) and were analyzed using GraphPad Prism software 8.1.0 (GraphPad Software, San Diego, CA, USA, www.graphpad.com). Data were tested for normal distribution using the Kolmogorov-Smirnov test. Continuous variables with normal distributions were analyzed with the Student's *t*-test, and data with non-normal distributions were analyzed with the Mann-Whitney *U* test. One-way analysis of variance was applied to compare the differences among multiple groups, followed by the Bonferroni post hoc test for pairwise comparison. Two-way analysis of variance was used to analyze the mean difference over time across groups and, when the results indicated significant differences, Bonferroni *post hoc* tests were applied.

## Results

**Tat-CX3CL1 (357–395aa) reduces cerebral edema and regulates the microglial polarization shift from an M1 to an M2 phenotype in the acute stroke phase**

We previously showed that Tat-CX3CL1 (357–395aa) reduced tissue loss caused by stroke using TTC staining (Zhang et al., 2021). Here, we assessed the effect of the peptide on whole-brain ischemic volume (**Figure 2A**) and confirmed that the peptide inhibits cerebral tissue loss. Tat-CX3CL1 (357–395aa) also significantly attenuated cerebral edema (**Figure 2B**) at 24 hours after MCAO and decreased mNSS scores at 1 and 3 days after MCAO ($P < 0.05$, **Figure 2C**).

To explore the potential function of Tat-CX3CL1 (357–395aa) in ischemic stroke, we first detected the expression of M1/M2-type inflammatory factors at different time points after ischemia/reperfusion. The results showed that expression of TNF-α (an M1-type inflammatory factor) increased 6 hours after stroke and peaked at 24 hours (**Additional Figure 1B**), while the levels of other cytokines, including inducible nitric oxide synthase (iNOS) and IL-1β, also peaked at 24 hours after stroke (**Additional Figure 1A** and **C**). However, the levels of M2-type inflammatory factors (CD-163, IL-10, and vascular endothelial growth factor [VEGF]) decreased 3 hours after stroke and remained stable until 24 hours (**Additional Figure 1D–F**). CD163 and IL-10 levels increased from 48 hours after stroke (**Additional Figure 1D** and **E**). Therefore, we selected the 24-hour I/R time point to investigate microglia polarization.

PCR analysis of cytokine production showed that Tat-CX3CL1 (357–395aa) inhibited the production of M1-type pro-inflammatory factors (iNOS, TNF-α, and IL-1β) (**Figure 3A–C**) and increased the levels of M2-type anti-inflammatory factors (IL-10, CD163, and VEGF) 24 hours after stroke (**Figure 3D–F**). Immunofluorescence assay of M1-type microglia (Iba1 and CD68 double-staining) in the cortex and striatum around the infarct area after 24 hours of reperfusion showed that the number of M1 microglia was significantly decreased in the Tat-CX3CL1 (357–395aa) group, not only in cortex but also in the striatum (**Figure 4A–D**). These data suggest that Tat-CX3CL1 (357–395aa) affects the microglia M1/M2 phenotype switch during ischemic stroke.

**Tat-CX3CL1 (357–395aa) inhibits sCX3CL1 generation**

CX3CL1 is localized on neurons and exists in membrane-anchored (mCX3CL1) and soluble (sCX3CL1) isoforms (Bajetto et al., 2002). mCX3CL1 is cleaved into sCX3CL1 by ADAM10 and ADAM17 (Garton et al., 2001; Clark et al., 2007). To elucidate the mechanism by which Tat-CX3CL1 (357–395aa) regulates microglia polarization, we first tested the effect of Tat-CX3CL1 (357–395aa) on the generation of sCX3CL1 and found that the peptide inhibits its formation **Figure 3G**). Furthermore, the ADAM17 inhibitor GW280264x not only inhibited the expression of pro-inflammatory cytokines, including iNOS, TNF-α, and IL-1β, and facilitated the expression of anti-inflammatory cytokines, including IL-10, CD-163, and VEGF (**Figure 5A–F**), but also reduced the production of sCX3CL1 (**Figure 3G**).

**Tat-CX3CL1 (357–395aa) promotes recovery of cognitive function after stroke by improving the integrity of myelinated fibers**

White matter injury after stroke can lead to cognitive deficit, neuroinflammation, demyelination, and axon degeneration (Rosenzweig and Carmichael, 2015; Shi et al., 2015; Wang et al., 2016). To explore whether Tat-CX3CL1 (357–395aa) could mitigate cognitive dysfunction, we performed a Morris water maze test and found that the peptide reduced escape latency and increased the time spent in the target quadrant, but it did not affect swimming speed (**Figure 6A–D**). Next, we evaluated whether Tat-CX3CL1 (357–395aa) could improve white matter integrity in stroke by double-staining for MBP and neurofilament H non-phosphorylated (SMI32) to evaluate white matter lesions. The immunofluorescence intensity of MBP staining was decreased in the corpus callosum and cortex at 35 days after MCAO (**Figure 7A–D**). However, Tat-CX3CL1 (357–395aa) markedly inhibited myelin loss. The SMI32/MBP ratio was used to assess damage to the myelin sheath and white matter. The results showed that the SMI32/MBP ratio in corpus callosum and cortex regions increased markedly in the I/R and DMSO groups compared with the sham group, but decreased in the Tat-CX3CL1 (357–395aa) group compared with the I/R and DMSO groups (**Figure 7A**, **B**, **E**, and **F**).

**Tat-CX3CL1 (357–395aa) reduces post-stroke anxiety and depression**

Post-stroke depression and anxiety exacerbate cognitive dysfunction, so we suspected that the mechanism underlying these effects might be related to microglia polarization. To test this, we evaluated anxiety-like behavior and depression using the open field test and the elevated plus maze, respectively. As is shown in **Figure 8**, compared with the I/R group and the DMSO group, the number of entrances into the open arm and the amount of time spent in the open arm were significantly increased in the Tat-CX3CL1 (357–395aa) mice (peptide group *versus* I/R group, $P < 0.0001$; peptide group *versus* DMSO group, $P < 0.001$).

Additionally, Tat-CX3CL1 (357–395aa) markedly increased the frequency of mice entering the central area and the amount of time spent in the central area in the open field test (**Figure 8D–F**). These results suggested that Tat-CX3CL1 (357–395aa) reduced post-stroke anxiety and depression.

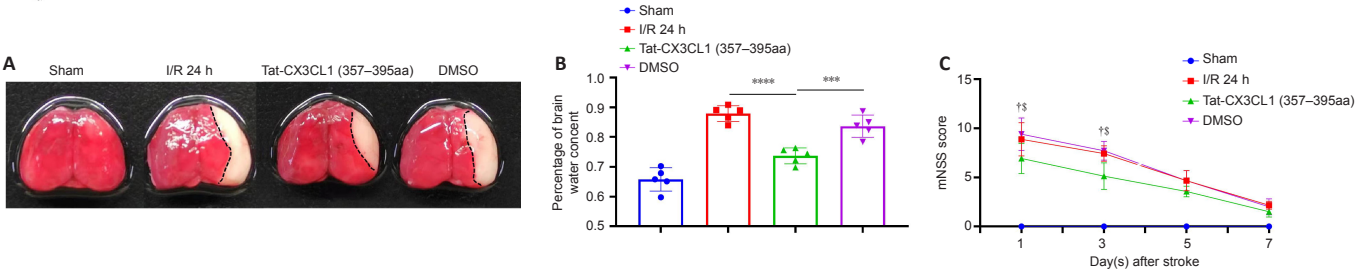


**Figure 2** | **Tat-CX3CL1 (357–395aa) reduces brain edema and improves neurological function in mice after cerebral infarction.**
(A) Tat-CX3CL1 (357–395aa) reduced infarct volume. Normal tissue is stained red, and infarcted tissue is stained white. (B) Tat-CX3CL1 (357–395 aa) reduced the water content of brain tissues after infarction. ***$P$ < 0.001, ****$P$ < 0.0001 (one-way analysis of variance followed by Bonferroni *post hoc* test), $n$ = 5/group. (C) mNSSs showed a gradual improvement in neurological function after cerebral infarction in the Tat-CX3CL1 (357–395 aa) group. †$P$ < 0.05, Tat-CX3CL1 (357–395aa) group *vs.* I/R group; $$P$ < 0.05, Tat-CX3CL1 (357–395aa) group *vs*. DMSO group (two-way analysis of variance followed by Bonferroni *post hoc* test), $n$ = 8–17/group. The experiments were repeated in triplicate. Data are expressed as the mean ± SEM. CX3CL1: C-X3-C motif chemokine ligand 1; DMSO: dimethyl sulfoxide; I/R: ischemic/reperfusion; mNSS: modified neurological function score.

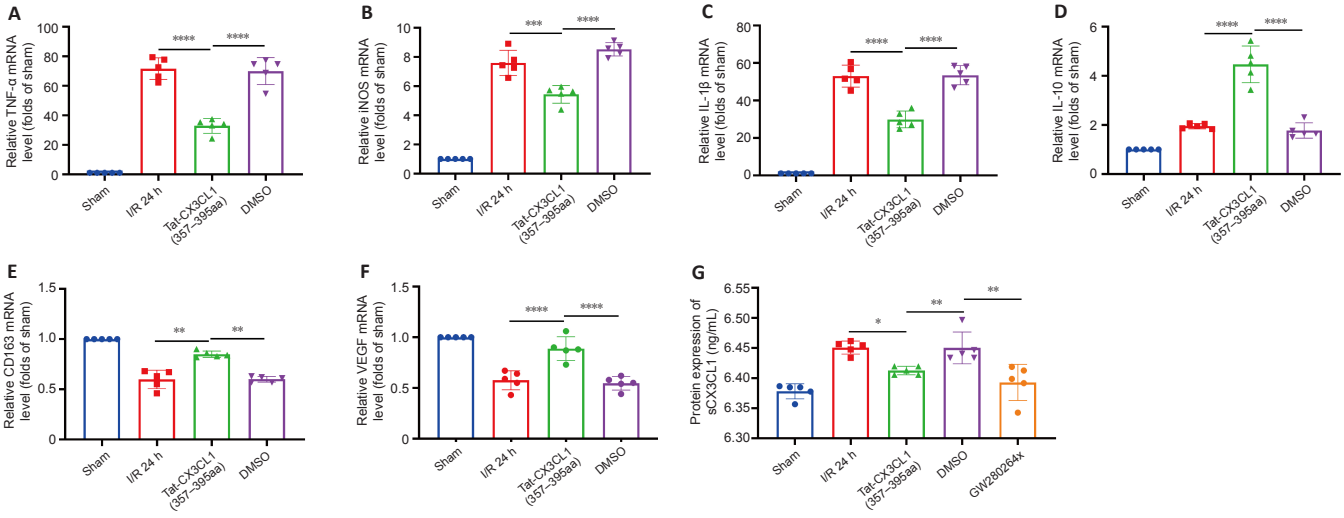


**Figure 3** | **Effects of Tat-CX3CL1 (357–395aa) on phenotypic polarization of M1/M2 microglia in ischemic brain tissue (qRT-PCR).**
(A–F) Tat-CX3CL1 (357–395 aa) reduced TNF-α, iNOS, and IL-1β mRNA expression levels (A–C) and increased IL-10, CD163, and VEGF mRNA expression levels (D–F) 24 hours after middle cerebral artery occlusion. (G) Tat-CX3CL1 (357–395aa) at a concentration of 10 μg/μL and GW280264x at a concentration of 1.5 μg/μL concentration decreased sCX3CL1 production 6 hours after middle cerebral artery occlusion (enzyme-linked immunosorbent assay). *$P$ < 0.05, **$P$ < 0.01, ***$P$ < 0.001, ****$P$ < 0.0001 (one-way analysis of variance followed by Bonferroni *post hoc* test), $n$ = 5/group. The experiments were repeated in triplicate. Data are expressed as the mean ± SEM. ADAM: A distintegrin and metalloproteinase; CX3CL1: C-X3-C motif chemokine ligand 1; DMSO: dimethyl sulfoxide; GW280264x: ADAM17 inhibitor; I/R: ischemia/reperfusion; IL-10: interleukin-10; IL-1β: interleukin-1β; iNOS: inducible nitric oxide synthase; TNF-α: tumor necrosis factor-α; VEGF: vascular endothelial growth factor.

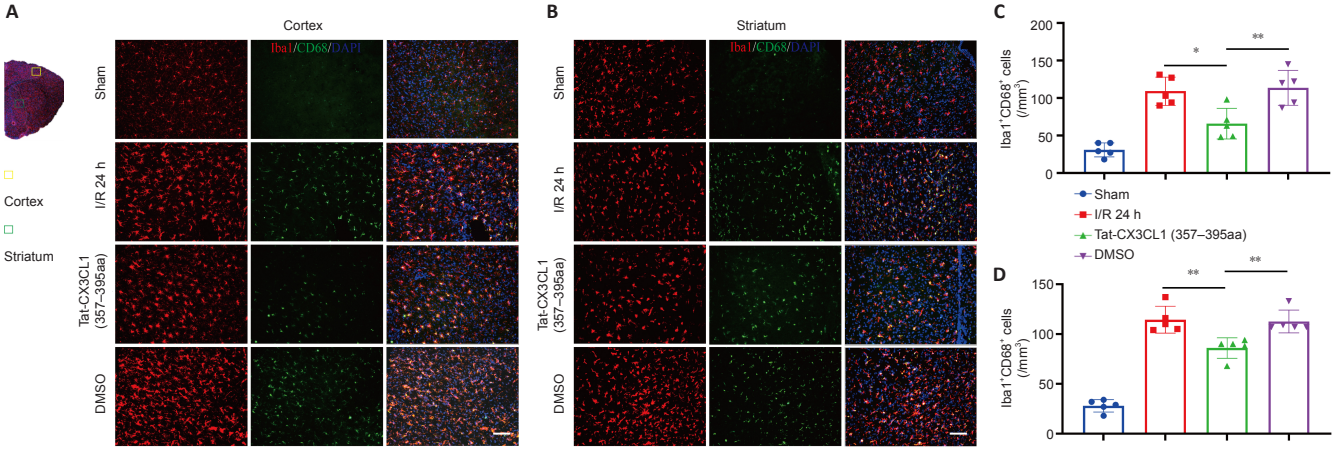


**Figure 4** | **Tat-CX3CL1 (357–395aa) inhibits microglia polarization to an M1 phenotype 24 hours after middle cerebral artery occlusion.**
(A, B) Representative images of Iba1 (red) and CD68 (green) immunostaining in the cortex and striatum. Scale bars: 50 μm. Selected areas were observed in the cortex and striatum. Thirty fields were recorded at each site, including the cortex, striatum, or corpus callosum. (C, D) Quantification of the number of Iba1$^+$ CD68$^+$ cells in the peri-infarct areas of the cortex and striatum. *$P$ < 0.05, **$P$ < 0.01 (one-way analysis of variance followed by Bonferroni *post hoc* test), $n$ = 5/group. The experiment was repeated at least three times. CX3CL1: C-X3-C motif chemokine ligand 1; DMSO: dimethyl sulfoxide; I/R: ischemia/reperfusion.

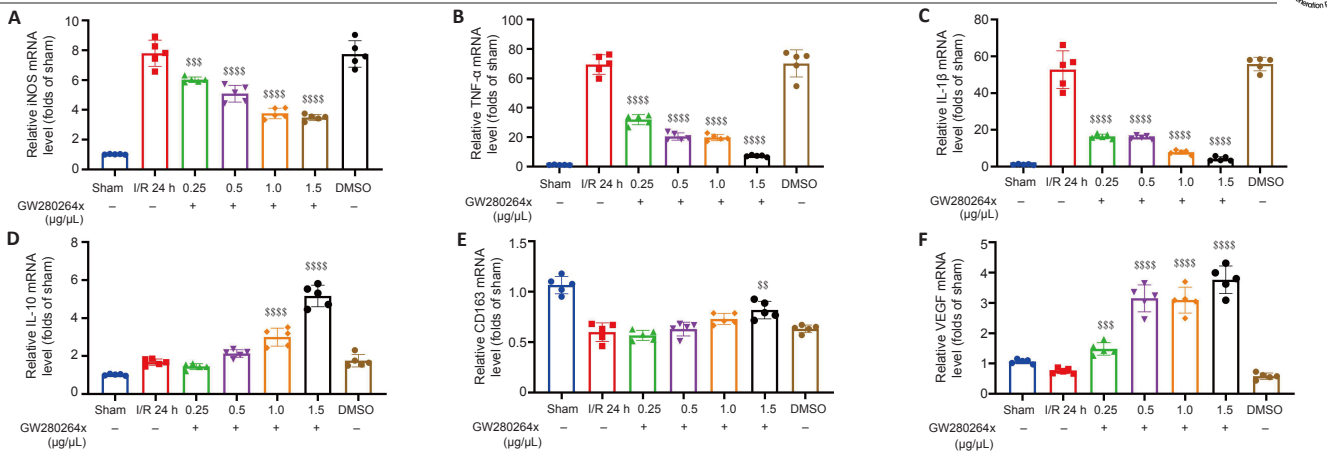


**Figure 5 | ADAM17 inhibitor GW280264x facilitates a phenotypic shift from M1 to M2 24 hours after middle cerebral artery occlusion.**
In these experiments, the mRNA expression of cytokines in cerebral infarcted tissue was determined in real-time RT-PCR after treatment with different concentrations (0.25, 0.5, 1.0, 1.5 μg/μL) of GW280264x. (A–F) GW280264x (0.25, 0.5, 1.0, and 1.5 μg/μL) decreased iNOS, TNF-α, and IL-1β mRNA expression levels (A–C) and increased CD163, IL-10, and VEGF mRNA expression levels (D–F). $$$P < 0.01, $$$P < 0.001, $$$$P < 0.0001, *vs.* DMSO group (two-way analysis of variance followed by Bonferroni *post hoc* test), *n* = 5/group. The experiment was repeated at least three times. ADAM: A distintegrin and metalloproteinase; DMSO: dimethyl sulfoxide; GW280264x: ADAM17 inhibitor; I/R: ischemia/reperfusion; IL-10: interleukin-10; IL-1β: interleukin-1β; iNOS: inducible nitric oxide synthase; TNF-α: tumor necrosis factor-α; VEGF: vascular endothelial growth factor.

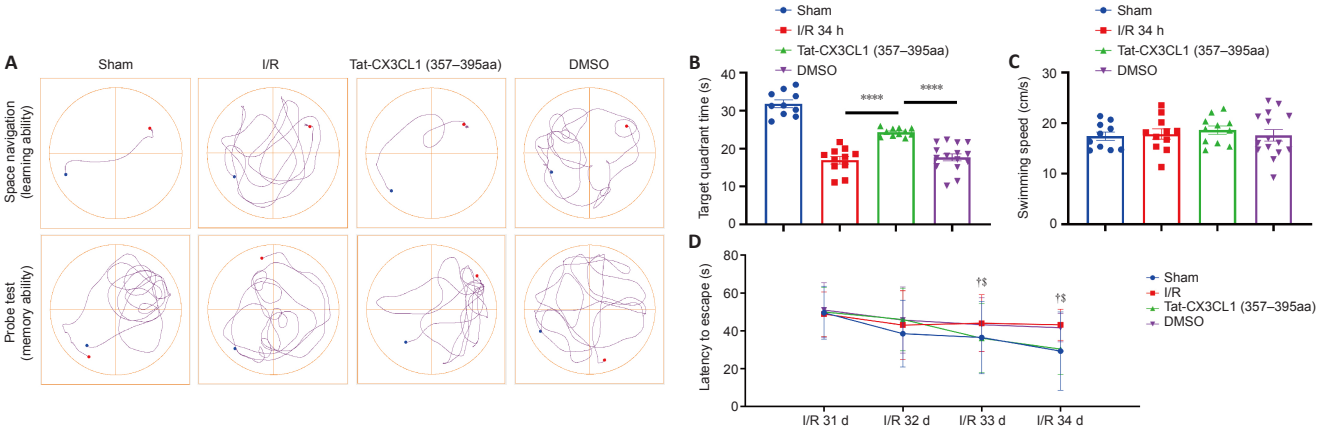


**Figure 6 | Tat-CX3CL1 (357–395aa) reduces long-term cognitive function impairment after middle cerebral artery occlusion (Morris water maze test).**
Long-term cognitive function evaluated by the Morris water maze test 31–34 days after middle cerebral artery occlusion. The time needed to reach the platform and the time the mice spent in the target quadrant in 1 minute were recorded at 34 days after middle cerebral artery occlusion, with repeated training before and after surgery. (A) Representative images of the swim paths in each group while the platform was present (learning phase) or absent (memory phase). *n* = 10–15/group. (B) Tat-CX3CL1 (357–395 aa) increased the time spent in the target quadrant (during the memory phase). (C) There was no change in swimming speed among the groups. (D) Tat-CX3CL1 (357–395 aa) significantly reduced the escape latency in mice (during the learning phase). Data are expressed as the mean ± SEM. ****P < 0.0001. †P < 0.05, Tat-CX3CL1 (357–395aa) group *vs.* I/R group; $P < 0.05, Tat-CX3CL1 (357–395aa) group *vs.* DMSO group (one-way analysis of variance followed by Bonferroni *post hoc* test in B and C, two-way analysis of variance followed by Bonferroni *post hoc* test in D). CX3CL1: C-X3-C motif chemokine ligand 1; DMSO: dimethyl sulfoxide; I/R: ischemia/reperfusion.

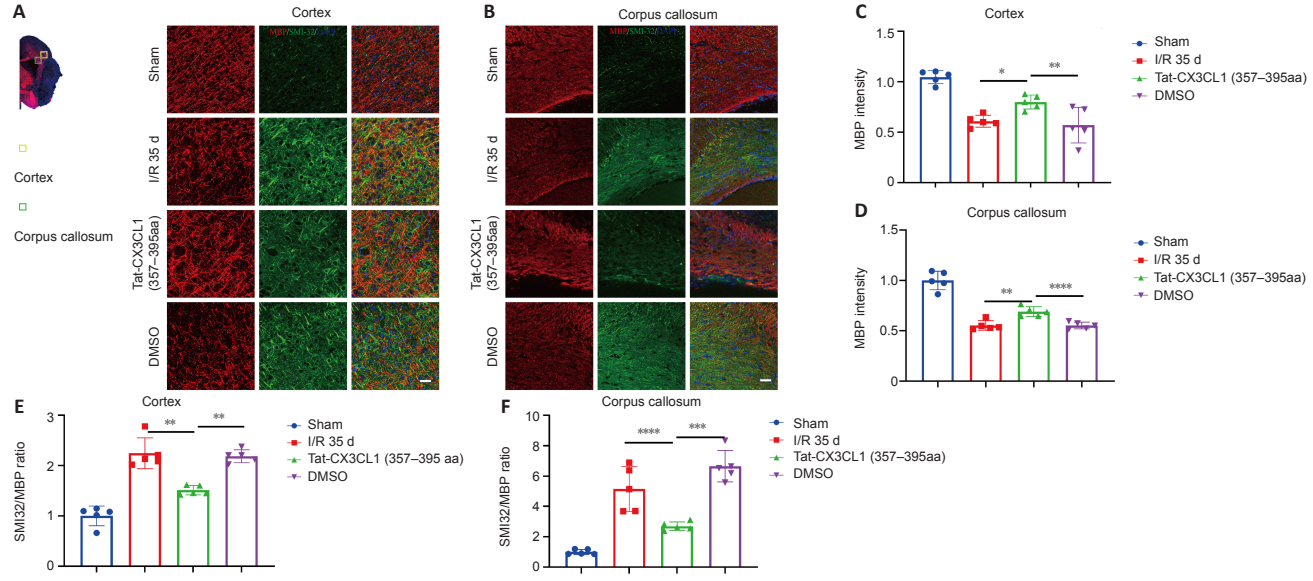


**Figure 7 | Tat-CX3CL1 (357–395aa) reduced white matter injury after MCAO.**
Double immunostaining for MBP and SMI32 at 35 days after MCAO or sham operation. Representative images of MBP (red) and SMI32 (green) double-immunostaining of peri-infarct areas in the cortex (A) and corpus callosum (B) from the sham and 35 days after MCAO, DMSO, and Tat-CX3CL1 (357–395aa) groups. Selected areas were observed in the cortex and striatum. MBP fluorescence intensity in the cortex (C) and corpus callosum (D). The ratio of SMI32 to MBP immunofluorescence intensity in the cortex (E) and corpus callosum (F). Scale bars: 100 μm. *n* = 5/group. *P < 0.05, **P < 0.01, ***P < 0.001, ****P < 0.0001 (one-way analysis of variance followed by Bonferroni *post hoc* test). CC: Corpus callosum; CX3CL1: C-X3-C motif chemokine ligand 1; DMSO: dimethyl sulfoxide; I/R: ischemia/reperfusion; MBP: myelin basic protein; MCAO: middle cerebral artery occlusion; SMI32: neurofilament H non-phosphorylated.

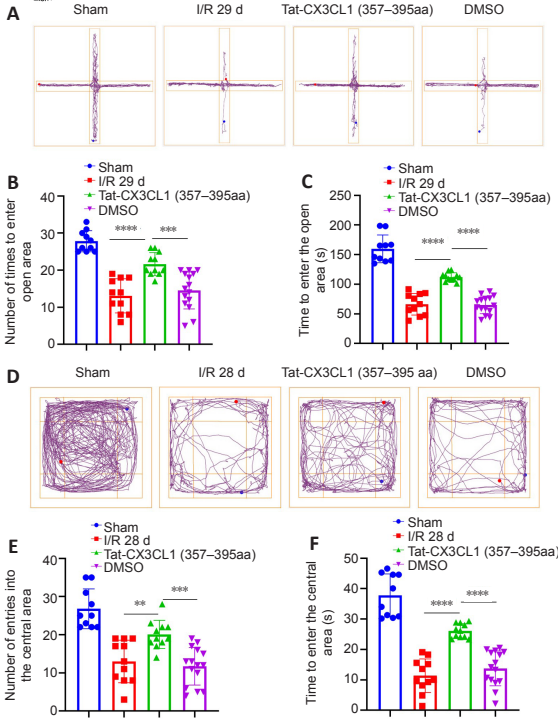


**Figure 8 | Tat-CX3CL1 (357–395aa) alleviates anxiety and depression in mice after middle cerebral artery occlusion.**

(A) Representative images of movement paths in the elevated plus maze for each group. The number of entries and the time spent in each arm were recorded for 5 minutes after training for 1 week. (B, C) Tat-CX3CL1 (357–395aa) increased the number of entries into the open arm and the time spent in the open arm. (D) Representative images of movement paths in the open field test. After training for 1 week, the number of entries into and time spent in the central area of the open field were recorded. (E, F) Tat-CX3CL1 (357–395aa) increased the number of entries and the time spent in each arm in the elevated plus maze test. $^{**}P < 0.01$, $^{***}P < 0.001$, $^{****}P < 0.0001$ (one-way analysis of variance followed by Bonferroni *post hoc* test), $n$ = 10–15/group. CX3CL1: C-X3-C motif chemokine ligand 1; DMSO: dimethyl sulfoxide; I/R: ischemia/reperfusion.

## Discussion

In the present study, we found that Tat-CX3CL1 (357–395aa) exerts a protective effect in the context of ischemic infarction by blocking the interaction between PSD-93 and CX3CL1 and reducing the production of soluble CX3CL1, resulting in inhibition of communication between neurons and microglia. Furthermore, we found that the peak expressions values of pro-inflammatory cytokines (M1-like) and anti-inflammatory cytokines (M2-like) differed. Thus, we propose that the peptide Tat-CX3CL1 (357–395aa) inhibits pro-inflammatory cytokine secretion and promotes anti-inflammatory cytokine expression in acute ischemia-reperfusion due to a polarization shift from an M1 phenotype to an M2 phenotype (**Figure 9**). Furthermore, Tat-CX3CL1 (357–395aa) diminished neurological impairment and improved long-term cognitive function after stroke. Collectively, these data demonstrate the beneficial effects of Tat-CX3CL1 (357–395aa) and suggest that the peptide may be a useful therapeutic agent for patients with ischemic stroke.

Accumulating evidence shows that microglia are polarized into different states within hours following the onset of stroke. Differential polarization of microglia to the classic pro-inflammatory type (M1-like) or the alternative protective type (M2-like) is activated at different stages, and can play detrimental or beneficial roles (Mabuchi et al., 2000; Lakhan et al., 2009; Hu et al., 2012). Furthermore, previous studies have indicated that the peak time points for cytokine expression are different in different microglia polarization states (Hu et al., 2012; Zhang et al., 2015; Ma et al., 2017). In addition to IL-10 and VEGF, CD163 is increasingly recognized as being associated with anti-inflammatory signals (D.Rajan, et al., 2020; Van Gorp et al., 2010). Thus, in this study, we selected several representative cytokines and detected their expression at different points during the reperfusion time course. The molecular mechanism underlying microglia polarization during stroke remains to be elucidated.

In this study, we reported the status of M1/M2-like microglia activation at different stages after stroke. M1-like microglia were activated 6 hours after stroke, peaked at 24 hours, and then persisted for several days, consistent with the peak expression of sCX3CL1 (Zhang et al., 2021), indicating that sCX3CL1 production promotes M1-like microglia activation. Conversely, M2-like microglia were suppressed at 24 hours following stroke. In addition, we found that Tat-CX3CL1 (357–395aa) facilitated microglia polarization from an M1 to an M2 phenotype by inhibiting M1-type cytokines (iNOS, TNF-α, and IL-1β) and promoting M2-type cytokines (CD-163, IL-10, and VEGF) at 24 hours after stroke.

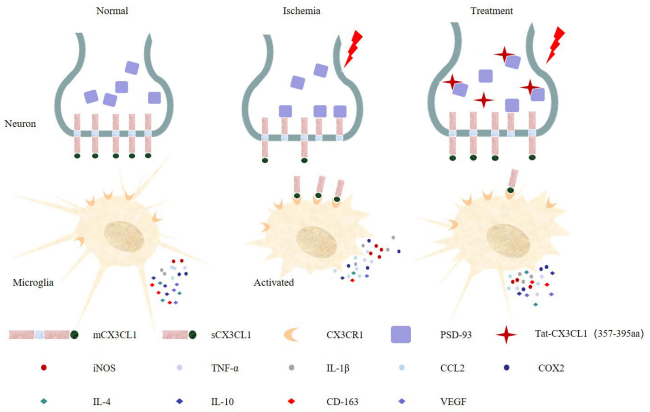


**Figure 9 | Schematic diagram of the neuroprotective effects of Tat-CX3CL1 (357–395aa) during cerebral ischemia/reperfusion.**

Tat-CX3CL1 (357–395aa) blocked PSD-93 binding to CX3CL1, inhibited the generation of soluble CX3CL1, and promoted the microglial phenotypic polarization from M1 type to M2 type. CCL2: Chemokine (C-C motif) ligand 2; Cox2: cyclooxygenase 2; CX3CL1: C-X3-C motif chemokine ligand 1; IL-4: interleukin-4; IL-10: interleukin-10; IL-1β: interleukin-1β; iNOS: inducible nitric oxide synthase; mCX3CL1: membrane-anchored CX3CL1; PSD-93: postsynaptic density-93; sCX3CL1: soluble CX3CL1; TNF-α: tumor necrosis factor-alpha; VEGF: vascular endothelial growth factor.

Previously, we reported that PSD-93 bound to CX3CL1 through amino acids 420–535 of PSD-93 and amino acids 357–395 of CX3CL1. Therefore, on the basis of these previous findings, we designed the peptide Tat-CX3CL1 (357–395aa) to block the binding of PSD-93 to CX3CL1 (Zhang et al., 2021). CX3CL1/CX3CR1 signaling is crucial for microglia-neuron cross-talk (Mizuno et al., 2003; Pabon et al., 2011; Shan et al., 2011; Lee et al., 2014; Febinger et al., 2015; Luo et al., 2019). In addition, PSD-93 binding to CX3CL1 facilitates the generation of sCX3CL1, which then binds to the CX3CR1 receptor expressed on microglia (Zhang et al., 2021). We found that Tat-CX3CL1 (357–395aa) reduced the release of soluble CX3CL1 and inhibited the expression of pro-inflammatory (M1-like) cytokines, suggesting that Tat-CX3CL1 (357–395aa) suppressed soluble CX3CL1 expression and inhibited CX3CL1/CX3CR1 signaling.

Previous studies have revealed that CX3CL1-CX3CR1 signaling regulates synaptic plasticity and cognitive function (Meucci et al., 2000; Deiva et al., 2004; Limatola et al., 2005; Ragozzino et al., 2006). Ischemic stroke impacts not only gray matter but also white matter and induces cognitive deficits in memory and learning. Furthermore, the incidence of post-stroke anxiety and depression is approximately 36.7% within 2 weeks after stroke (Pérez-Piñar et al., 2017; Rafsten et al., 2018). In this study, we showed that Tat-CX3CL1 (357–395aa) promoted white matter repair and cognitive improvement. Additionally, we found that Tat-CX3CL1 (357–395aa) had a potentially beneficial role on post-stroke anxiety and depression. These results suggest that inhibition of microglial polarization in the acute stage of ischemic infarction could help restore nerve function in later stages, and that Tat-CX3CL1 (357–395aa) is an attractive therapeutic agent for stroke. However, while the peptide may help treat post-stroke cognitive impairment, the delivery method limits its feasibility with regards to real-world application. In recent years, with the development of nanotechnology, increasingly more peptide-based nanoparticle treatments administered via an intranasal delivery route are being used in neuroscience research, increasing the possibility of using Tat-CX3CL1 (357–395aa) clinically in the future.

The present study focused on central inflammation and did not address peripheral inflammation. Furthermore, only a few representative cytokines or chemokines were selected to assess M1/M2 phenotypes, and the reason for the two significant peaks in iNOS expression at 24 and 72 hours following stroke remains unclear. To further elucidate the mechanism underlying the effect of the PSD-93-CX3CL1 interaction on microglia phenotypic transformation, further investigations should be carried out in knockout mice, and the dynamic changes in microglia morphology should be explored *in vivo*.

In conclusion, our findings indicated that Tat-CX3CL1 (357–395aa) inhibits the generation of soluble CX3CL1, promotes microglia M2-type polarization, and exerts neuroprotective effects in a mouse model of ischemic stroke. Thus, the Tat-CX3CL1 (357–395aa) peptide might be a potential therapeutic agent for ischemic stroke.

**Author contributions:** *QXZ designed and performed the experiments, and drafted the manuscript. LQR interpreted the data and edited the manuscript. XWC conducted the experiments, analyzed the data, and drafted the manuscript. HY performed the experiments and analyzed the data. LPK, JJS and SYL conducted the experiments and analyzed the data. XML conceived the experiments, interpreted the data and edited the manuscript. All authors approved the final manuscript.*
**Conflicts of interest:** *None of the authors has any potential conflict of interest.*
**Author statement:** *This paper has been posted as a preprint on Research Square with doi: https://doi.org/10.21203/rs.3.rs-538353/v1, which*

*is available from: https://assets.researchsquare.com/files/rs-538353/v1/7cf9f653-30e3-4295-9a38-100a7cf1dd8b.pdf?c=1631883305.*

**Availability of data and materials:** *All data generated or analyzed during this study are included in this published article and its supplementary information files.*



**Additional file:**

***Additinal Figure 1:*** *Expression of M1/M2 inflammatory cytokines in mice after middle cerebral artery occlusion.*

## References

Bajetto A, Bonavia R, Barbero S, Schettini G (2002) Characterization of chemokines and their receptors in the central nervous system: physiopathological implications. J Neurochem 82:1311-1329.

Chen J, Li X, Xu S, Zhang M, Wu Z, Zhang X, Xu Y, Chen Y (2020) Delayed PARP-1 inhibition alleviates post-stroke inflammation in male versus female mice: differences and similarities. Front Cell Neurosci 14:77.

Clark AK, Yip PK, Grist J, Gentry C, Staniland AA, Marchand F, Dehvari M, Wotherspoon G, Winter J, Ullah J, Bevan S, Malcangio M (2007) Inhibition of spinal microglial cathepsin S for the reversal of neuropathic pain. Proc Natl Acad Sci U S A 104:10655-10660.

Deiva K, Geeraerts T, Salim H, Leclerc P, Héry C, Hugel B, Freyssinet JM, Tardieu M (2004) Fractalkine reduces N-methyl-d-aspartate-induced calcium flux and apoptosis in human neurons through extracellular signal-regulated kinase activation. Eur J Neurosci 20:3222-3232.

Donatti AF, Soriano RN, Leite-Panissi CR, Branco LG, de Souza AS (2017) Anxiolytic-like effect of hydrogen sulfide (H(2)S) in rats exposed and re-exposed to the elevated plus-maze and open field tests. Neurosci Lett 642:77-85.

Dreymueller D, Martin C, Kogel T, Pruessmeyer J, Hess FM, Horiuchi K, Uhlig S, Ludwig A (2012) Lung endothelial ADAM17 regulates the acute inflammatory response to lipopolysaccharide. EMBO Mol Med 4:412-423.

Febinger HY, Thomasy HE, Pavlova MN, Ringgold KM, Barf PR, George AM, Grillo JN, Bachstetter AD, Garcia JA, Cardona AE, Opp MR, Gemma C (2015) Time-dependent effects of CX3CR1 in a mouse model of mild traumatic brain injury. J Neuroinflammation 12:154.

Fumagalli M, Lombardi M, Gressens P, Verderio C (2018) How to reprogram microglia toward beneficial functions. Glia 66:2531-2549.

Garton KJ, Gough PJ, Blobel CP, Murphy G, Greaves DR, Dempsey PJ, Raines EW (2001) Tumor necrosis factor-alpha-converting enzyme (ADAM17) mediates the cleavage and shedding of fractalkine (CX3CL1). J Biol Chem 276:37993-38001.

Gelderblom M, Leypoldt F, Steinbach K, Behrens D, Choe CU, Siler DA, Arumugam TV, Orthey E, Gerloff C, Tolosa E, Magnus T (2009) Temporal and spatial dynamics of cerebral immune cell accumulation in stroke. Stroke 40:1849-1857.

Gülke E, Gelderblom M, Magnus T (2018) Danger signals in stroke and their role on microglia activation after ischemia. Ther Adv Neurol Disord 11:1756286418774254.

Hu X, Li P, Guo Y, Wang H, Leak RK, Chen S, Gao Y, Chen J (2012) Microglia/macrophage polarization dynamics reveal novel mechanism of injury expansion after focal cerebral ischemia. Stroke 43:3063-3070.

Hu X, Leak RK, Shi Y, Suenaga J, Gao Y, Zheng P, Chen J (2015) Microglial and macrophage polarization—new prospects for brain repair. Nat Rev Neurol 11:56-64.

Jin R, Liu L, Zhang S, Nanda A, Li G (2013) Role of inflammation and its mediators in acute ischemic stroke. J Cardiovasc Transl Res 6:834-851.

Kraeuter AK, Guest PC, Sarnyai Z (2019) The elevated plus maze test for measuring anxiety-like behavior in rodents. Methods Mol Biol 1916:69-74.

Lakhan SE, Kirchgessner A, Hofer M (2009) Inflammatory mechanisms in ischemic stroke: therapeutic approaches. J Transl Med 7:97.

Lee S, Xu G, Jay TR, Bhatta S, Kim KW, Jung S, Landreth GE, Ransohoff RM, Lamb BT (2014) Opposing effects of membrane-anchored CX3CL1 on amyloid and tau pathologies via the p38 MAPK pathway. J Neurosci 34:12538-12546.

Limatola C, Lauro C, Catalano M, Ciotti MT, Bertollini C, Di Angelantonio S, Ragozzino D, Eusebi F (2005) Chemokine CX3CL1 protects rat hippocampal neurons against glutamate-mediated excitotoxicity. J Neuroimmunol 166:19-28.

Liu X, Liu J, Zhao S, Zhang H, Cai W, Cai M, Ji X, Leak RK, Gao Y, Chen J, Hu X (2016) Interleukin-4 is essential for microglia/macrophage M2 polarization and long-term recovery after cerebral ischemia. Stroke 47:498-504.

Luo P, Chu SF, Zhang Z, Xia CY, Chen NH (2019) Fractalkine/CX3CR1 is involved in the cross-talk between neuron and glia in neurological diseases. Brain Res Bull 146:12-21.

Ma Y, Wang J, Wang Y, Yang GY (2017) The biphasic function of microglia in ischemic stroke. Prog Neurobiol 157:247-272.

Mabuchi T, Kitagawa K, Ohtsuki T, Kuwabara K, Yagita Y, Yanagihara T, Hori M, Matsumoto M (2000) Contribution of microglia/macrophages to expansion of infarction and response of oligodendrocytes after focal cerebral ischemia in rats. Stroke 31:1735-1743.

Meucci O, Fatatis A, Simen AA, Miller RJ (2000) Expression of CX3CR1 chemokine receptors on neurons and their role in neuronal survival. Proc Natl Acad Sci U S A 97:8075-8080.

National Research Council (2011) Guide for the Care and Use of Laboratory Animals, 8th Edition. Washington, DC: The National Academies Press.

Mizuno T, Kawanokuchi J, Numata K, Suzumura A (2003) Production and neuroprotective functions of fractalkine in the central nervous system. Brain Res 979:65-70.

Pabon MM, Bachstetter AD, Hudson CE, Gemma C, Bickford PC (2011) CX3CL1 reduces neurotoxicity and microglial activation in a rat model of Parkinson's disease. J Neuroinflammation 8:9.

Paxinos G, Franklin KBJ (2013) Paxinos and Franklin's the mouse brain in stereotaxic coordinates. 4th ed. Boston: Elsevier/Academic Press.

Percie du Sert N, Hurst V, Ahluwalia A, Alam S, Avey MT, Baker M, Browne WJ, Clark A, Cuthill IC, Dirnagl U, Emerson M, Garner P, Holgate ST, Howells DW, Karp NA, Lazic SE, Lidster K, MacCallum CJ, Macleod M, Pearl EJ, et al. (2020) The ARRIVE guidelines 2.0: Updated guidelines for reporting animal research. PLoS Biol 18:e3000410.

Pérez-Piñar M, Ayerbe L, González E, Mathur R, Foguet-Boreu Q, Ayis S (2017) Anxiety disorders and risk of stroke: A systematic review and meta-analysis. Eur Psychiatry 41:102-108.

Qi W, Cao D, Li Y, Peng A, Wang Y, Gao K, Tao C, Wu Y (2018) Atorvastatin ameliorates early brain injury through inhibition of apoptosis and ER stress in a rat model of subarachnoid hemorrhage. Biosci Rep 38:BSR20171035.

Qin C, Zhou LQ, Ma XT, Hu ZW, Yang S, Chen M, Bosco DB, Wu LJ, Tian DS (2019) Dual functions of microglia in ischemic stroke. Neurosci Bull 35:921-933.

Rafsten L, Danielsson A, Sunnerhagen KS (2018) Anxiety after stroke: A systematic review and meta-analysis. J Rehabil Med 50:769-778.

Ragozzino D, Di Angelantonio S, Trettel F, Bertollini C, Maggi L, Gross C, Charo IF, Limatola C, Eusebi F (2006) Chemokine fractalkine/CX3CL1 negatively modulates active glutamatergic synapses in rat hippocampal neurons. J Neurosci 26:10488-10498.

Rong R, Yang H, Rong L, Wei X, Li Q, Liu X, Gao H, Xu Y, Zhang Q (2016) Proteomic analysis of PSD-93 knockout mice following the induction of ischemic cerebral injury. Neurotoxicology 53:1-11.

Rosenzweig S, Carmichael ST (2015) The axon-glia unit in white matter stroke: mechanisms of damage and recovery. Brain Res 1623:123-134.

Schneider CA, Rasband WS, Eliceiri KW (2012) NIH Image to ImageJ: 25 years of image analysis. Nat Methods 9:671-675.

Shan S, Hong-Min T, Yi F, Jun-Peng G, Yue F, Yan-Hong T, Yun-Ke Y, Wen-Wei L, Xiang-Yu W, Jun M, Guo-Hua W, Ya-Ling H, Hua-Wei L, Ding-Fang C (2011) New evidences for fractalkine/CX3CL1 involved in substantia nigral microglial activation and behavioral changes in a rat model of Parkinson's disease. Neurobiol Aging 32:443-458.

Shi H, Hu X, Leak RK, Shi Y, An C, Suenaga J, Chen J, Gao Y (2015) Demyelination as a rational therapeutic target for ischemic or traumatic brain injury. Exp Neurol 272:17-25.

Van Gorp H, Delputte PL, Nauwynck HJ (2010) Scavenger receptor CD163, a Jack-of-all-trades and potential target for cell-directed therapy. Mol Immunol 47(7-8):1650-1660.

Wang J, Xing H, Wan L, Jiang X, Wang C, Wu Y (2018) Treatment targets for M2 microglia polarization in ischemic stroke. Biomed Pharmacother 105:518-525.

Wang Y, Liu G, Hong D, Chen F, Ji X, Cao G (2016) White matter injury in ischemic stroke. Prog Neurobiol 141:45-60.

Zhang M, Li Q, Chen L, Li J, Zhang X, Chen X, Zhang Q, Shao Y, Xu Y (2014) PSD-93 deletion inhibits Fyn-mediated phosphorylation of NR2B and protects against focal cerebral ischemia. Neurobiol Dis 68:104-111.

Zhang Q, Cheng H, Rong R, Yang H, Ji Q, Li Q, Rong L, Hu G, Xu Y (2015) The effect of PSD-93 deficiency on the expression of early inflammatory cytokines induced by ischemic brain injury. Cell Biochem Biophys 73:695-700.

Zhang Q, Zhu W, Xu F, Dai X, Shi L, Cai W, Mu H, Hitchens TK, Foley LM, Liu X, Yu F, Chen J, Shi Y, Leak RK, Gao Y, Chen J, Hu X (2019) The interleukin-4/PPARγ signaling axis promotes oligodendrocyte differentiation and remyelination after brain injury. PLoS Biol 17:e3000330.

Zhang Q, Yang H, Gao H, Liu X, Li Q, Rong R, Liu Z, Wei XE, Kong L, Xu Y, Rong L (2020) PSD-93 interacts with SynGAP and promotes SynGAP ubiquitination and ischemic brain injury in mice. Transl Stroke Res 11:1137-1147.

Zhang Q, He L, Chen M, Yang H, Cao X, Liu X, Hao Q, Chen Z, Liu T, Wei XE, Rong L (2021) PSD-93 mediates the crosstalk between neuron and microglia and facilitates acute ischemic stroke injury by binding to CX3CL1. J Neurochem 157:2145-2157.

*C-Editor: Zhao M; S-Editor: Li CH; L-Editors: Li CH, Song LP; T-Editor: Jia Y*

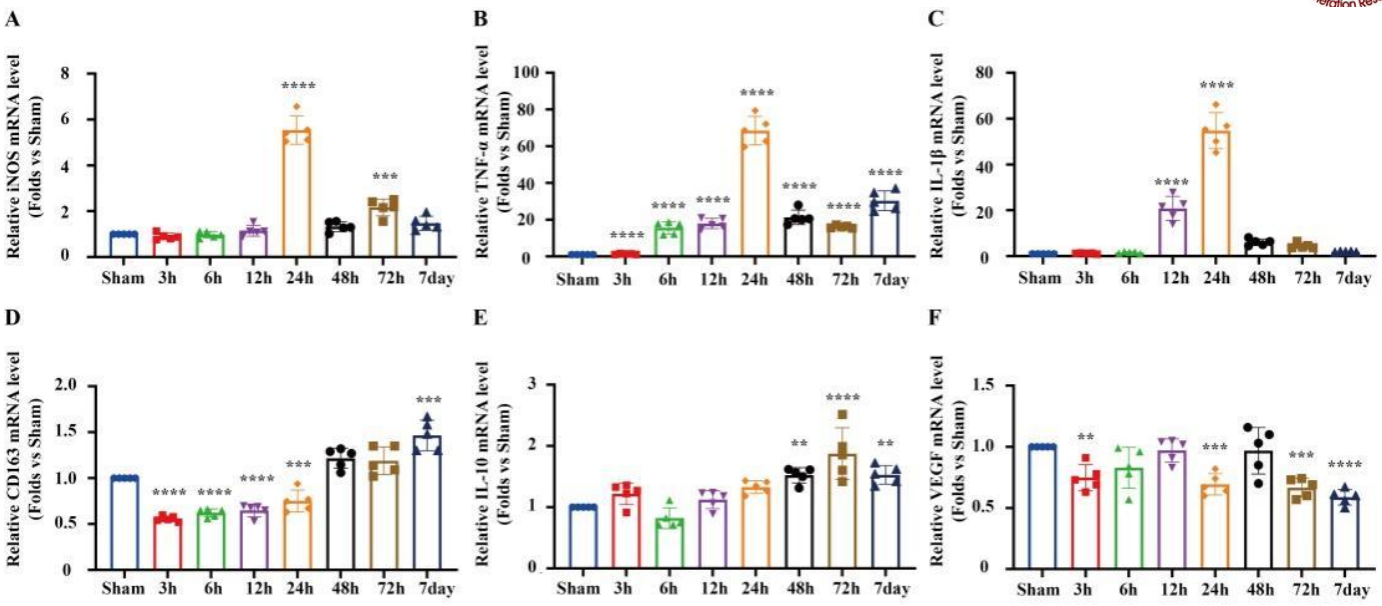


**Additional Figure 1 Expression of M1/M2 inflammatory cytokines in mice after middle cerebral artery occlusion.**

(A-F) The expression of iNOS (A), TNF-α (B) and IL-1β (C), and CD163 (D), IL-10 (E) and VEGF (F) at sham, 3, 6, 12, 24, 48, and 72 hours, and 7 days after middle cerebral artery occlusion. Data are expressed as the mean ± SEM. $^{**}P < 0.01$, $^{***}P < 0.001$, $^{****}P < 0.0001$, *vs*. sham group (one-way analysis of variance followed by Bonferroni *post hoc* test). n=5/group. The experiments were repeated for 3 times. IL-1β: Interleukin-1β; IL-10: interleukin-10; iNOS: inducible nitric oxide synthase; TNF-α: tumor necrosis factor-α; VEGF: vascular endothelial growth factor.